The antiferromagnetic spin-$^{1/2}$ chain with competing dimers and plaquettes: numerical versus exact results

1998 J. Phys.: Condens. Matter 10 3635

(http://iopscience.iop.org/0953-8984/10/16/015)

J. Phys.: Condens. Matter **10** (1998) 3635–3649. Printed in the UK PII: S0953-8984(98)88040-5

The antiferromagnetic spin-1/2 chain with competing dimers and plaquettes: numerical versus exact results

J Richter†, N B Ivanov‡ and J Schulenburg†

† Institut für Theoretische Physik, Universität Magdeburg, PO Box 4120, D-39016 Magdeburg, Germany

‡ Institute for Solid State Physics, Sofia, Bulgaria

Received 1 October 1997, in final form 5 January 1998

Abstract. We examine the ground state and the excitations of a one-dimensional Heisenberg spin-1/2 antiferromagnet with alternating dimers and four-spin plaquettes (a dimer–plaquette chain). The properties of the system depend on the competing dimer and plaquette bonds. Several exact, exact numerical and perturbational results are presented. We find that the system is gapped for all parameter values. The spin pair correlation functions can be characterized by three different correlation lengths for dimer–dimer, dimer–plaquette and plaquette–plaquette correlations. For the latter we find an effective $S = 1$ Haldane-like behaviour in the limit of dominating dimer bonds.

On introducing frustration, the system undergoes a first-order phase transition to a fully dimerized state. As regards the phase relationships of the ground-state wave function, the system represents an example showing exact validity of the Marshall–Peierls sign rule in a strongly frustrated antiferromagnet.

The model considered is related to the recently found 1/5-depleted square-lattice Heisenberg system CaV_4O_9.

1. Introduction

The exciting collective magnetic properties of low-dimensional quantum spin systems have attracted much attention over the last decade. The search for systems with spin-liquid ground states is one subject of continuous interest. Compressible (gapped) and incompressible (gapless) spin-liquid phases with more or less exotic ground-state ordering have been discussed in particular for the frustrated J_1–J_2 model on the square lattice (see e.g. [1]).

The recent discovery of a spin gap in $S = 1/2$ quasi-two-dimensional CaV_4O_9 [2, 3] has stimulated the investigation of quantum disorder and gap formation of systems with different types of antiferromagnetic nearest-neighbour (NN) bond [4–10]. CaV_4O_9 has a layered structure where the magnetic V^{4+} ions have spin 1/2 and form a 1/5-depleted square lattice [11, 12]. The minimal model for CaV_4O_9 is a 1/5-depleted Heisenberg model, i.e. a model with four-spin plaquettes connected at their edges with one neighbouring plaquette. Because of the distortion of the lattice [11, 12] the intra-plaquette J_p-bonds and the inter-plaquette (dimer) J_d-bonds might be different. Though in a classical version of this non-frustrated Heisenberg model the Néel state is the stable ground state for any $J_p > 0$, $J_d > 0$, in the quantum case a competition arises between a local singlet formation of a couple of spins along a dimer bond J_d and a local singlet formation of the four spins belonging to a plaquette and coupled by J_p. However, the explanation of the measured spin gap by competition between J_p and J_d would require unreasonably large differences between J_p

0953-8984/98/163635+15$19.50

and J_d. As proposed in several papers [13, 12, 14–17] one needs additional frustration to get reasonable values for the gap.

In this paper we extend our preliminary discussion [9, 10] of the competition between dimer and plaquette bonds and the role of frustration in the one-dimensional counterpart of the depleted square-lattice Heisenberg model. This model is simpler than the 2D model, but nevertheless it contains non-trivial physics. As far as we are aware, currently there is no corresponding quasi-1D material, but it seems to be possible that it may be synthesized in the future.

Though the Heisenberg model considered is a spin-1/2 model, it will be shown below that the model also contains elements of the physics of the spin-1 chain which is currently also under intensive discussion (see e.g. [18–21] and references therein).

The paper is organized as follows. In section 2 we present the model and elaborate on some exact statements concerning eigenvalues and eigenstates of the model. In section 3 we discuss exact numerical data for chains of up to 32 sites as well as analytic results obtained using perturbation theory. Conclusions are given in section 4.

2. The model and general results

The spin-1/2 Heisenberg chain considered here consists of N spins forming $N_p = N/4$ plaquettes which are connected by $N_d = N_p$ dimer bonds (see figure 1). The two spins connected by the nth dimer bond J_d we call dimer spins and denote them by $\boldsymbol{S}_\alpha^n$ and $\boldsymbol{S}_\beta^n$, where the index α (β) stands for the left-hand (right-hand) spin. The two spins sited at the top and the bottom of the nth plaquette we call plaquette spins and denote them by $\boldsymbol{S}_a^n$ and $\boldsymbol{S}_b^n$, where the index a (b) stands for the top (bottom) spin. With this notation we write the Hamiltonian as

$$H_{d-p} = J_d \sum_{n=1}^{N_p} \boldsymbol{S}_\alpha^n \cdot \boldsymbol{S}_\beta^n + J_p \sum_{n=1}^{N_p} (\boldsymbol{S}_\beta^n \cdot \boldsymbol{S}_a^n + \boldsymbol{S}_\beta^n \cdot \boldsymbol{S}_b^n + \boldsymbol{S}_a^n \cdot \boldsymbol{S}_\alpha^{n+1} + \boldsymbol{S}_b^n \cdot \boldsymbol{S}_\alpha^{n+1}) \tag{1}$$

($J_d, J_p > 0$). Frustration is introduced by a diagonal antiferromagnetic bond J_f connecting a top and a bottom plaquette spin (see figure 1). Then the total Hamiltonian reads

$$H = H_{d-p} + H_f = H_{d-p} + J_f \sum_{n=1}^{N_p} \boldsymbol{S}_a^n \cdot \boldsymbol{S}_b^n \qquad J_f \geqslant 0. \tag{2}$$

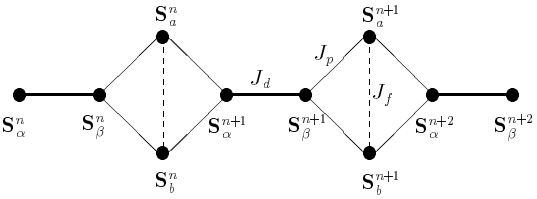

Figure 1. See the text.

For the sake of convenience we consider chains with periodic boundary conditions.

Approximately at the same time as we introduced [9] the above-defined dimer–plaquette chain, Takano and co-workers [22] considered a so-called diamond chain, built of plaquettes only. The ground-state problem of this diamond chain was recently analysed by Niggemann *et al* [23]. The main difference between the two models consists in the existence of the

dimer bond in the dimer–plaquette chain. As a consequence, the two models belong to different universality classes. We will briefly discuss some important differences between the two models in section 4.

For the above described dimer–plaquette chain, equations (1), (2), we can make the general statements given below in subsections 2.1–2.9.

2.1. The classical ground state

For $J_f < J_p$ the ground state is a Néel state. The correlations are $\langle \boldsymbol{S}_a^n \cdot \boldsymbol{S}_b^n \rangle = +S^2$ between a bottom and top spin of the same plaquette (J_f-bonds), $\langle \boldsymbol{S}_\alpha^n \cdot \boldsymbol{S}_\beta^n \rangle = -S^2$ between two neighbouring dimer spins (J_d-bonds) and $\langle \boldsymbol{S}_\beta^n \cdot \boldsymbol{S}_{a(b)}^n \rangle = \langle \boldsymbol{S}_\alpha^{n+1} \cdot \boldsymbol{S}_{a(b)}^n \rangle = -S^2$ between a dimer spin and a neighbouring plaquette spin (J_p-bonds). For $J_f > J_p$ the ground state has twisted plaquette spins. The corresponding correlations of neighbouring spins are $\langle \boldsymbol{S}_a^n \cdot \boldsymbol{S}_b^n \rangle = S^2(2J_p^2/J_f^2 - 1)$, $\langle \boldsymbol{S}_\alpha^n \cdot \boldsymbol{S}_\beta^n \rangle = -S^2$ and $\langle \boldsymbol{S}_\beta^n \cdot \boldsymbol{S}_{a(b)}^n \rangle = \langle \boldsymbol{S}_\alpha^{n+1} \cdot \boldsymbol{S}_{a(b)}^n \rangle = -S^2 J_p/J_f$.

Now we turn to the quantum spin-1/2 case.

2.2. Integrals of motion

In addition to the usual integrals of motion (the z-component and the square of the total spin) there are N_p local integrals of motion, namely the square of the total spin of the top and bottom spin of a plaquette n, i.e.

$$[H, (\boldsymbol{S}_{ab}^n)^2]_- = 0 \qquad \boldsymbol{S}_{ab}^n = \boldsymbol{S}_a^n + \boldsymbol{S}_b^n. \tag{3}$$

Hence we can classify all eigenstates in terms of the following set of the quantum numbers: energy E, the z-component of the total spin M, the square of the total spin S and N_p local quantum numbers S_p^n of $(\boldsymbol{S}_{ab}^n)^2$, where the values for S_p^n are 0 (singlet) or 1 (triplet). For the correlation function of a top and a bottom spin of plaquette n we have $\langle \boldsymbol{S}_a^n \cdot \boldsymbol{S}_b^n \rangle = -3/4$ $(+1/4)$ for $S_p^n = 0$ ($S_p^n = 1$).

2.3. The Lieb–Mattis theorem and the ground state in the non-frustrated limit

In the limit $J_f = 0$, i.e. $H = H_{p-d}$, the lattice is bipartite and the Lieb–Mattis theorem is valid [24, 25], i.e. the ground state is a singlet, $S = 0$, of the total spin. As a consequence of the theorem we have $\langle \boldsymbol{S}_a^n \cdot \boldsymbol{S}_b^n \rangle > 0$ since the top and bottom spins of a plaquette n belong to the same sublattice, i.e. the ground state is a singlet of the total spin but all local quantum numbers are $S_p^n = 1$ ($n = 1, \ldots, N_p$).

We notice that the numerical results (see below) indicate that the ground state is a singlet of the total spin for finite frustration, too, which is in accordance with other calculations of the ground state of various frustrated antiferromagnets.

2.4. Mapping onto a spin-1/2–spin-1 chain

As a result of the statement made in subsection 2.3 for zero temperature, the Hamiltonian (1) can be exactly mapped onto a chain with mixed spin-1/2 and spin-1 objects as shown in figure 2.

This effective model describes not only the ground state, but also all other eigenstates of (1) with $S_p^n = 1$ for all $n = 1, \ldots, N_p$.

Notice that the antiferromagnetic chain with alternating spins $S = 1/2$ and $S = 1$ was recently discussed as a quantum ferrimagnet [26–28]; however, the effective model here is of a different kind, since we have twice as many spins $S = 1/2$ as spins $S = 1$.

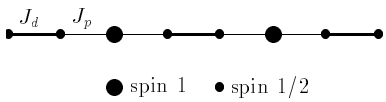

Figure 2. A spin-1/2–spin-1 chain, which is equivalent to the non-frustrated Hamiltonian (1) for zero temperature.

2.5. Product eigenstates

We consider now the class of eigenstates which do not correspond to the spin-1/2–spin-1 chain, i.e. we consider states where some of the local quantum numbers S_p^n are zero. Suppose $S_p^i = 0$ in the plaquette i. Then the top and bottom spins of plaquette i form a singlet which is decoupled from all other spins, i.e. we have $\langle \boldsymbol{S}_{a(b)}^n \cdot \boldsymbol{S}_{a(b)}^i \rangle = 0$ $(n \neq i)$ and $\langle \boldsymbol{S}_{\alpha(\beta)}^n \cdot \boldsymbol{S}_{a(b)}^i \rangle = 0$. Hence the eigenstate can be written in product form:

$$|\Psi\rangle = |(a_i, b_i)\rangle |\Psi_{\text{remainder}}\rangle \tag{4}$$

where $|(a_i, b_i)\rangle = (\uparrow_{a_i}\downarrow_{b_i} - \downarrow_{a_i}\uparrow_{b_i})/\sqrt{2}$ is a pair singlet state of the top and bottom spins of plaquette i and $|\Psi_{\text{remainder}}\rangle$ is a state describing all of the remaining $N-2$ spins forming a corresponding open chain with dimer ends. Suppose $S_p^i = 0$ in $L > 1$ plaquettes i. Then the eigenstate separates into L pair singlet states of the top and bottom spins of plaquettes i and eigenstates of the finite chain pieces lying between two plaquettes with $S_p^i = 0$. The more plaquettes i in a singlet state $S_p^i = 0$, the shorter the finite chain pieces between two plaquettes with $S_p^i = 0$. The extreme case is the state with $S_p^n = 0$ for all $n = 1, \ldots, N_p$ plaquettes, where the finite pieces between two plaquettes are just the dimers themselves. This state can be explicitly written as

$$|\Psi_{0,\ldots,0}\rangle = \prod_{n=1}^{N_p} |(a_n, b_n)\rangle \prod_{n=1}^{N_p} |(\alpha_n, \beta_n)\rangle \tag{5}$$

where $|(\alpha_n, \beta_n)\rangle = (\uparrow_{\alpha_n}\downarrow_{\beta_n} - \downarrow_{\alpha_n}\uparrow_{\beta_n})/\sqrt{2}$ is a pair singlet state of a dimer bond n. The energy of this state is

$$E_{0,\ldots,0} = -\frac{3}{4} J_d N_p - \frac{3}{4} J_f N_p. \tag{6}$$

2.6. Eigenstates and energy levels—the frustrated versus the non-frustrated model

Between the eigenstates and the energy of the non-frustrated (1) and the frustrated (2) models there exist simple relations due to the fact that H_{p-d} commutes with H_f. Hence the eigenfunctions of H_{p-d} are not changed on including frustration, and for the energy contribution of the frustrating part H_f only the local quantum numbers S_p^n are important. Consider any eigenstate of H_{p-d} with energy E_{p-d}, and N_p^s plaquettes with quantum number $S_p^n = 0$ and N_p^t plaquettes with quantum number $S_p^i = 1$ $(N_p^t + N_p^s = N_p)$. Then the energy for the frustrated model $H = H_{p-d} + H_f$ is

$$E_{p-d,f} = E_{p-d} + J_f\left(\frac{1}{4}N_p^t - \frac{3}{4}N_p^s\right) = E_{p-d} + J_f\left(\frac{1}{4}N_p - N_p^s\right). \tag{7}$$

2.7. Upper and lower bounds for the critical J_f^c

From equation (7) it is obvious that J_f favours energetically the singlet formation of plaquette spins, and for large J_f the singlet product state (5) becomes the ground state of H.

According to subsection 2.3 the ground state is the lowest eigenstate with $S_p^n = 1$ for all $n = 1, \ldots, N_p$ for $J_f = 0$ and has the energy $E^0_{1,\ldots,1}$. Following the ideas of reference [23] we used a linear programming scheme to prove that at a critical value $J_f^c > 0$ a first-order transition takes place from this ground state directly to the product state (5) of energy $E_{0,\ldots,0}$, equation (6), with $S_p^n = 0$ for all $n = 1, \ldots, N_p$. Then the critical J_f^c is defined by $E^0_{1,\ldots,1}|_{J_f=J_f^c} = E_{0,\ldots,0}|_{J_f=J_f^c}$. According to (7) we have

$$E^0_{1,\ldots,1}|_{J_f=J_f^c} = E^0_{1,\ldots,1}|_{J_f=0} + \frac{1}{4}J_f^c N_p \stackrel{!}{=} -\frac{3}{4}(J_d + J_f^c)N_p$$

which yields

$$J_f^c = -\frac{3}{4}J_d - \frac{1}{N_p}E^0_{1,\ldots,1}\bigg|_{J_f=0}. \tag{8}$$

First we look for an upper bound for J_f^c. We consider $J_f \leqslant J_f^c$. Then the state with $S_p^n = 1$ for all $n = 1, \ldots, N_p$ is the ground state and $E_{0,\ldots,0}$, equation (6), sets an upper bound for the ground-state energy $E^0_{1,\ldots,1}$.

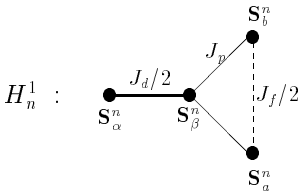

Figure 3. An elementary cluster H_n^1 for the decomposition $H = \sum(H_n^1 + H_n^2)$ (see the text). The cluster H_n^2 is the mirror image of H_n^1.

A lower bound of the ground-state energy is found (see for instance [30]) by a simple cluster decomposition of H:

$$\begin{aligned} H &= \sum_{n=1}^{N_p} H_n^1 + H_n^2 \\ H_n^1 &= \frac{J_d}{2}\boldsymbol{S}_\alpha^n \cdot \boldsymbol{S}_\beta^n + J_p \boldsymbol{S}_\beta^n \cdot (\boldsymbol{S}_a^n + \boldsymbol{S}_b^n) + \frac{J_f}{2}\boldsymbol{S}_a^n \cdot \boldsymbol{S}_b^n \\ H_n^2 &= \frac{J_f}{2}\boldsymbol{S}_a^n \cdot \boldsymbol{S}_b^n + J_p \boldsymbol{S}_\alpha^{n+1} \cdot (\boldsymbol{S}_a^n + \boldsymbol{S}_b^n) + \frac{J_d}{2}\boldsymbol{S}_\alpha^{n+1} \cdot \boldsymbol{S}_\beta^{n+1} \end{aligned} \tag{9}$$

(see figure 3). The lowest energy of H_n^1 and H_n^2 with $S_p^n = 1$ is

$$E_n = -\frac{J_d}{8} - \frac{J_p}{4} + \frac{J_f}{8} - \frac{1}{4}\sqrt{J_d^2 - 2J_dJ_p + 9J_p^2}. \tag{10}$$

The lower bound for $E^0_{1,\ldots,1}$ is $2N_pE_n$. The resulting inequality

$$-\frac{3}{4}(J_d + J_f)N_p \geqslant E^0_{1,\ldots,1} \geqslant 2N_pE_n$$

implies the following upper bound for J_f^c:

$$J_f^c \leqslant -\frac{J_d}{2} + \frac{J_p}{2} + \frac{1}{2}\sqrt{J_d^2 - 2J_dJ_p + 9J_p^2}. \tag{11}$$

Next we look for a lower bound for J_f^c. We use equation (8) and replace $E^0_{1,\ldots,1}(J_f = 0)$ by a variational energy E_{var} of a trial ground state of H_{p-d}. Since $E_{var} \geqslant E^0_{1,\ldots,1}(J_f = 0)$, the lower bound is

$$J_f^c \geqslant -\frac{3}{4}J_d - \frac{1}{N_p}E_{var}. \tag{12}$$

For $J_p > 0$ we are able to find a trial state (see section 3) with $E_{var} \leqslant -N_p\,\frac{3}{4}J_d$, i.e. $J_f^c \geqslant 0$ is valid for finite J_p.

2.8. Validity of the Marshall–Peierls sign rule in a frustrated spin system

In the limit $J_f = 0$ ($H = H_{p-d}$) the lattice is bipartite and the Marshall–Peierls sign rule is valid [31, 34], i.e. the phase relations of the ground-state wave function are exactly known. Though there are several arguments that indicate that this sign rule will survive a finite frustration [32–36], the validity of the sign rule in a non-bipartite frustrated lattice cannot be shown generally.

On the basis of the statements in subsections 2.6 and 2.7 we argue that for all $J_f < J_f^c$ ($J_f^c > 0$) the ground state of the frustrated Hamiltonian $H_{p-d} + H_f$ is equal to the ground state of the non-frustrated Hamiltonian H_{p-d}.

Hence the plaquette–dimer chain considered is one example where the Marshall–Peierls sign rule does indeed survive finite frustration.

2.9. The spin gap for large frustration, $J_f > J_f^c$

We consider the gap Δ of the first triplet excitation versus the singlet product ground state $|\Psi_{0,\ldots,0}\rangle$, equation (5). Since in $|\Psi_{0,\ldots,0}\rangle$ the top and bottom spins of any plaquette are separated from all other spins, the first triplet excitation is a state $|\Psi_{0,\ldots,0,1,0,\ldots,0}\rangle$ with one triplet for a certain plaquette i, i.e. $S_p^i = 1$:

$$|\Psi_{0,\ldots,1,0,\ldots,0}\rangle = |\Psi_{-<>-}\rangle \prod_{n=1}^{N_p-1} |(a_n, b_n)\rangle \prod_{n=1}^{N_p-2} |(\alpha_n, \beta_n)\rangle \tag{13}$$

where in $\prod_{n=1}^{N_p-1}$ the plaquette i is excluded and in $\prod_{n=1}^{N_p-2}$ the left-hand and right-hand neighbouring dimers of plaquette i are excluded. $|\Psi_{-<>-}\rangle$ represents just the state with $S_p^i = 1$ for the excluded plaquette i and the adjacent dimers i and $i+1$. The degeneracy of the state (13) is $3N_p$.

The excitation gap is the energy difference between the ground state $|\Psi_{0,\ldots,0}\rangle$, equation (5), and $|\Psi_{0,\ldots,0,1,0,\ldots,0}\rangle$, equation (13):

$$\Delta = E_1 - E_0 = \frac{3}{2}J_d + J_f + E_{-<>-}(J_d, J_p) \tag{14}$$

where $E_{-<>-}(J_d, J_p)$ is the energy of the excluded cluster $-<>-$ for $J_f = 0$. Obviously, $E_1 - E_0$ is independent of the size N. Since $|\Psi_{-<>-}\rangle$ is a state of only six spins it is no problem to calculate $E_{-<>-}(J_d, J_p)$, i.e. to find the exact value for $E_1 - E_0$.

3. Exact diagonalization versus perturbation theory

Using the Lanczos algorithm we calculate the ground state and several low-lying states for chains with periodic boundary conditions of size $N = 8, 16, 24, 32$ (i.e. $N_p = 2, 4, 6, 8$ plaquettes).

In the limits where $J_d/J_p \ll 1$ and $J_p/J_d \ll 1$ we calculate the energies of the singlet ground state and the first triplet excitation by second-order perturbation theory. In the limit where $J_d = 0$ the unperturbed ground state is a product of the lowest four-spin plaquette states. In the opposite limit ($J_p = 0$) the ground state of H_{p-d}, equation (1), is a product of dimer singlets and threefold-degenerate triplets of the plaquette spins. The perturbation theory in second order of J_p leads to the following effective spin Hamiltonian:

$$H_{eff} = -\frac{3}{4}J_d N_p - \frac{J_p^2}{J_d}N_p + \frac{J_p^2}{2J_d}\sum_{n=1}^{N_p} \boldsymbol{S}_{ab}^n \cdot \boldsymbol{S}_{ab}^{n+1} \tag{15}$$

where the quantities $\boldsymbol{S}_{ab}^n$ are spin-1 operators, i.e. $(\boldsymbol{S}_{ab}^n)^2 = 2$. We see that in the limit where $J_p/J_d \ll 1$, the dimer–plaquette $S = 1/2$ model maps onto the $S = 1$ Haldane chain with an effective exchange parameter $J_{eff} = J_p^2/2J_d$.

3.1. Ground-state energy, low-lying excitations, spin gap

First we consider the ground-state energy E_0. For large frustration $J_f \geqslant J_f^c$ the explicit expression for E_0 is given by equation (6).

For $J_f < J_f^c$ the ground-state energy obeys equation (7) and it is sufficient to consider the unfrustrated Hamiltonian H_{p-d}. First we consider the two limits of small dimer exchange $J_d \ll J_p$ and of small plaquette exchange $J_p \ll J_d$. In the first case the perturbation theory yields

$$\frac{E_0}{4N_p} = -J_p\left[\frac{1}{2} + \frac{1}{4}\frac{43}{576}\left(\frac{J_d}{J_p}\right)^2\right]. \tag{16}$$

The opposite limit is described by the effective spin-1 model (15), i.e.

$$\frac{E_0}{4N_p} = -\frac{3}{16}J_d - \frac{J_p^2}{4J_d} + \frac{J_p^2}{8J_d}\epsilon_H \tag{17}$$

where $\epsilon_H = -1.401\,484\,038\,971$ [18, 19] is the well-known energy per site of the Haldane chain.

The numerical data for $N = 16$ are shown in figure 4. The energies presented belong to the corresponding lowest eigenstate for a given set of local quantum numbers S_p^n, $n = 1, \ldots, 4$. (An exception is the state with total spin $S = 1$ and $S_p^n = 1$, $n = 1, \ldots, 4$, which is the first triplet excitation versus the singlet ground state.) The state with highest energy is just the product state $|\Psi_{0,\ldots,0}\rangle$, equation (5); its energy is independent of J_p (see equation (6)). All of the energies presented are degenerate for $J_p = 0$. On increasing J_p the energies exhibit a quadratic dependence on J_p for small J_p, and a linear dependence on J_p for larger J_p. Notice that the linear dependence on J_p (obtained via perturbation theory in the limit $J_p \gg J_d$; see (16)) is already well established for $J_p \approx J_d$.

In all of the finite systems ($N = 8, 16, 24, 32$) considered in this paper, the first triplet excitation has the same local quantum numbers as the ground state, i.e. $S_p^n = 1$ ($n = 1, \ldots, N_p$). The eigenstates with singlets $S_p^n = 0$ for some n have higher energies, and we find that the larger the number of plaquettes with $S_p^n = 0$ the higher the energy.

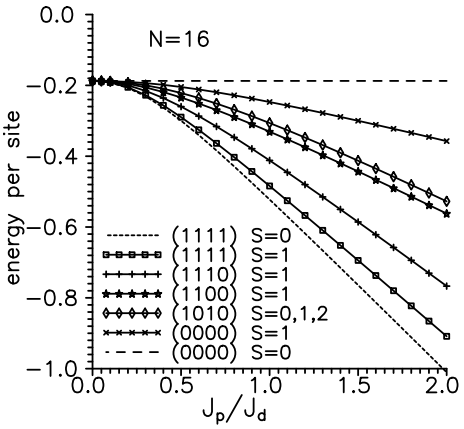

Figure 4. Energy eigenvalues versus J_p/J_d for the unfrustrated model H_{p-d} with $N = 16$ sites. The four numbers in brackets give the local quantum numbers S_p^n, $n = 1, \ldots, 4$; S is the quantum number of the total spin.

Next we consider the excitation gap Δ between the singlet ground state and the first triplet excitation. This triplet excitation is the lowest excitation of all (see figure 4). The perturbation theory for large J_p/J_d yields

$$\Delta = J_p\left[1 - \frac{1}{3}\frac{J_d}{J_p} - \frac{61}{576}\left(\frac{J_d}{J_p}\right)^2\right]. \tag{18}$$

This result was already obtained in [4]. In the opposite limit, $J_d/J_p \gg 1$, we can use the results for the Haldane chain [18, 19] and we have

$$\Delta = \frac{J_p^2}{2J_d}\Delta_H = 0.410\,50\frac{J_p^2}{2J_d}. \tag{19}$$

If we include frustration the situation is not changed for $J_f < J_f^c$ except in a small region in the vicinity of the transition, i.e. for $J_f \approx J_f^c$ the first excitation is not a triplet but a singlet indicating strong frustration effects [37]. For $J_f > J_f^c$ the gap is exactly known for the whole parameter range (see equation (14)).

Numerical data are shown in figure 5, where Δ is shown versus J_p. The linear and quadratic dependences for large and small J_p correspond to the perturbation theory (equations (18) and (19)). On the scale used for figure 5 the data for $N = 24$ and $N = 32$ almost coincide.

In the case of the unfrustrated dimer–plaquette chain with identical NN bonds $J_p = J_d = 1$ the gap is already about 50% larger than the Haldane gap Δ_H; that is, $\Delta_{N=24} = 0.609\,22$, $\Delta_{N=32} = 0.609\,06$, $\Delta_{N\to\infty} = 0.6086$. In accordance with 2D models for CaV_4O_9 the frustration may enlarge the gap; in the model considered we have $\Delta(J_f + x) \geqslant \Delta(J_f)$ $(x > 0)$.

Obviously, though we have a spin-1/2 chain, Δ is finite for any finite J_p which corresponds to the observation that the gapless spectrum of the Bethe chain is an exceptional case.

3.2. Critical J_f^c

The critical point J_f^c is defined in subsection 2.7. This point coincides with the point of maximal frustration indicated by a maximum in the ground-state energy versus J_f precisely

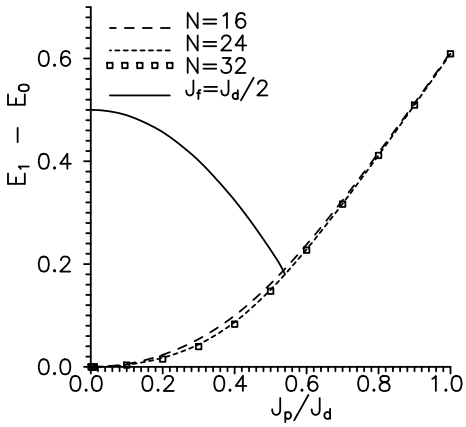

Figure 5. The excitation gap between the singlet ground state and the lowest triplet excitation. The dashed lines and the squares correspond to the unfrustrated case. The solid line corresponds to the frustrated case with $J_f > J_f^c$, where the gap is independent of N. For $J_f < J_f^c$ the gaps of the frustrated and the unfrustrated models coincide. The critical point for $N = 24$ is at $J_p = 0.534 J_d$.

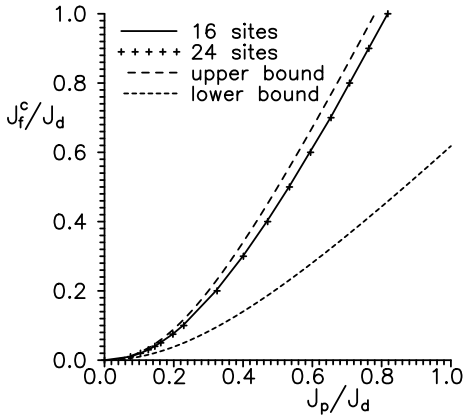

Figure 6. The critical frustration J_f^c versus J_p for $N = 24$ (crosses) and $N = 16$ (solid line) and upper and lower bounds (see the text). Above the critical line the ground state of H is the fully dimerized product state (5) and below the critical line the ground state of the total Hamiltonian H coincides with that of H_{p-d} (equation (1)).

at $J_f = J_f^c$.

Upper and lower bounds for J_f^c are given in equations (11) and (12).

For the estimation of the lower bound we consider a variational state of the form

$$|\Psi_{var}\rangle = \prod_{\substack{n=1 \\ n \text{ odd}}}^{N_p-1} |\uparrow_{a_n} \uparrow_{b_n}\rangle |\downarrow_{a_{n+1}} \downarrow_{b_{n+1}}\rangle |\{\alpha_n, \beta_n\}\rangle |\{\beta_{n+1}, \alpha_{n+1}\}\rangle \tag{20}$$

where $|\uparrow_{a_n} \uparrow_{b_n}\rangle$ ($|\downarrow_{a_{n+1}} \downarrow_{b_{n+1}}\rangle$) is a triplet state of the plaquette spins with z-component $S_{ab}^{n,z} = +1$ ($S_{ab}^{n+1,z} = -1$) and

$$|\{\alpha_n, \beta_n\}\rangle |\{\beta_{n+1}, \alpha_{n+1}\}\rangle$$
$$= (1 + x^2)^{-1} (|\uparrow_{\alpha_n} \downarrow_{\beta_n}\rangle - x|\downarrow_{\alpha_n} \uparrow_{\beta_n}\rangle)(|\uparrow_{\beta_{n+1}} \downarrow_{\alpha_{n+1}}\rangle - x|\downarrow_{\beta_{n+1}} \uparrow_{\alpha_{n+1}}\rangle)$$

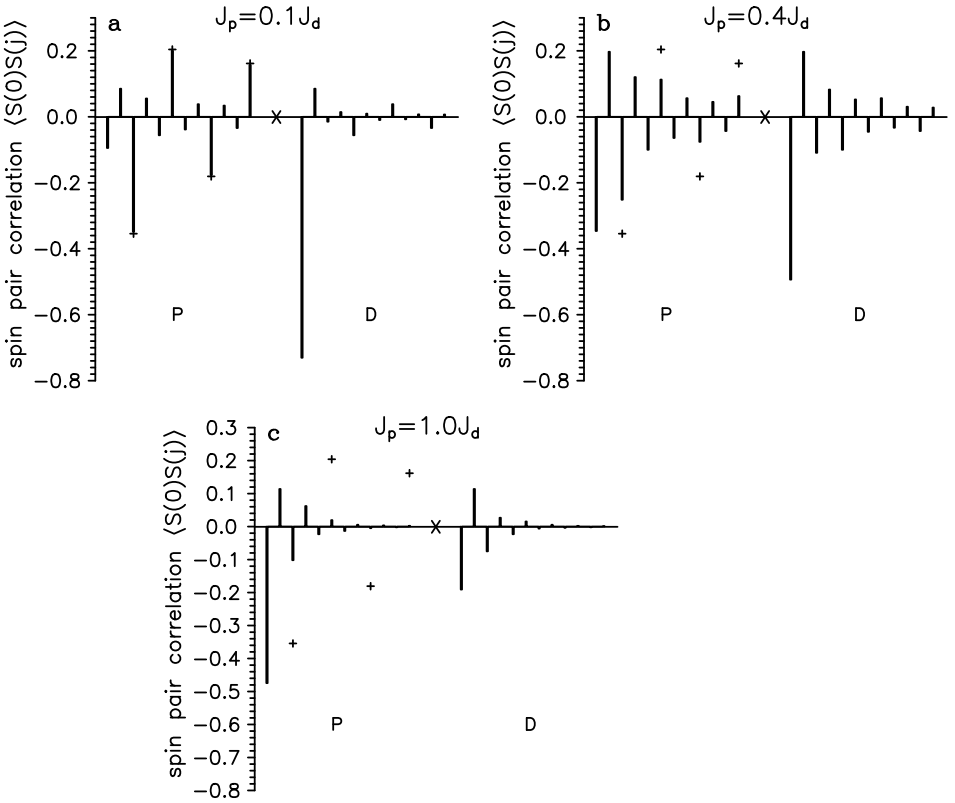

Figure 7. Spin pair correlations $\langle \boldsymbol{S}(0) \cdot \boldsymbol{S}(j) \rangle$ versus the separation of the unfrustrated chain H_{p-d} of length $N = 32$ sites for three values of J_p/J_d. For the spin–spin separation the number of NN steps from the reference spin at 0 to the spin at j is used. Left-hand (P) side of the figures: reference spin $\boldsymbol{S}(0)$ is a plaquette spin $\boldsymbol{S}^n_{a(b)}$, i.e. the correlations $j = 1, 2, 4, 5, 7, 8, 10, 11$ are plaquette–dimer correlations, the correlations $j = 3, 6, 9, 12$ are plaquette–plaquette correlations (cf. figure 1). Right-hand (D) side of the figures: reference spin $\boldsymbol{S}(0)$ is a dimer spin $\boldsymbol{S}^n_\alpha$, i.e. the correlations $j = 1, 3, 4, 6, 7, 9, 10, 12$ are dimer–dimer correlations, the correlations $j = 2, 5, 8, 11$ are dimer–plaquette correlations (cf. figure 1). The crosses indicate the correlations of the corresponding Haldane chain of length $N = 8$.

is a variational state which interpolates between a dimer singlet state ($x = 1$) and a Néel state ($x = 0$). The calculation of the optimized x is simple:

$$x = -2J_p/J_d + \sqrt{1 + 4J_p^2/J_d^2}.$$

The energy of this state E_{var} entering equation (12) is quite good in the limit of small J_p and becomes exact for $J_p = 0$.

The numerical results are presented in figure 6. While the lower bound demonstrates that J_f^c is finite for any finite J_p, we see that the expression (11) for the upper bound is close to the actual value of J_f^c and can serve as an approximative analytic expression for J_f^c.

3.3. Pair spin correlation and string order

At first we consider the limit of large frustrating $J_f > J_f^c$, where the simple product state $|\Psi_{0,\ldots,0}\rangle$, equation (5), is the ground state. Then all spin–spin correlations are zero except

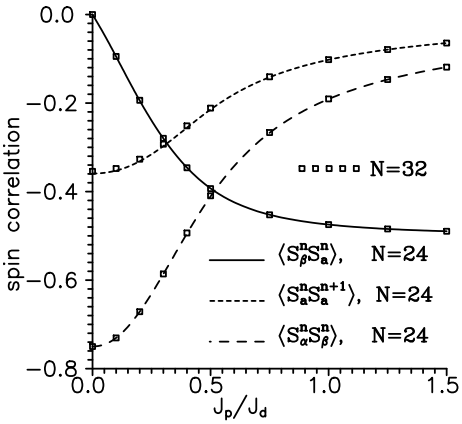

Figure 8. Short-range spin correlations versus J_p for the unfrustrated chain H_{p-d} and $N = 24$ sites. $\langle \boldsymbol{S}^n_\beta \cdot \boldsymbol{S}^n_{a(b)} \rangle$: NN dimer spin–plaquette spin; $\langle \boldsymbol{S}^n_a \cdot \boldsymbol{S}^{n+1}_a \rangle$: plaquette spin–plaquette spin of neighbouring plaquettes; $\langle \boldsymbol{S}^n_\alpha \cdot \boldsymbol{S}^n_\beta \rangle$: NN dimer spin–dimer spin.

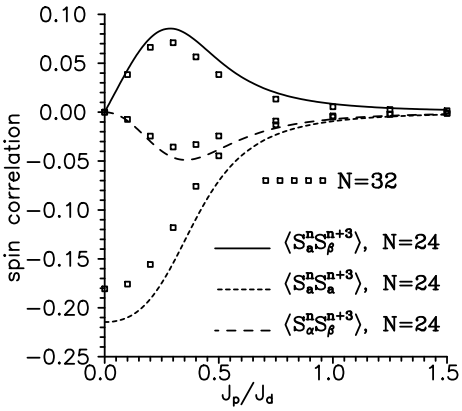

Figure 9. Spin correlations for largest spin separations versus J_p for the unfrustrated chain H_{p-d} and $N = 24$. $\langle \boldsymbol{S}^n_a \cdot \boldsymbol{S}^{n+3}_\beta \rangle$: dimer spin–plaquette spin; $\langle \boldsymbol{S}^n_a \cdot \boldsymbol{S}^{n+3}_a \rangle$: plaquette spin–plaquette spin; $\langle \boldsymbol{S}^n_\alpha \cdot \boldsymbol{S}^{n+3}_\beta \rangle$: dimer spin–dimer spin.

$\langle \boldsymbol{S}^n_\alpha \cdot \boldsymbol{S}^n_\beta \rangle$ and $\langle \boldsymbol{S}^n_a \cdot \boldsymbol{S}^n_b \rangle$ which take their extreme value $-3/4$.

In what follows we discuss the more interesting case where $J_f < J_f^c$, i.e. the ground state is that of the unfrustrated H_{p-d}. Numerical results for $N = 24$ and $N = 32$ are shown in figures 7–10. To get a general impression of the distance dependence of the correlations we present in figure 7 a histogram showing the pair correlation versus the separation for three values of J_p/J_d. The short-range correlations $\langle \boldsymbol{S}^n_\alpha \cdot \boldsymbol{S}^n_\beta \rangle$ (NN dimer spins), $\langle \boldsymbol{S}^n_\beta \cdot \boldsymbol{S}^n_{a(b)} \rangle$ (NN plaquette–dimer spins) and $\langle \boldsymbol{S}^n_{a(b)} \cdot \boldsymbol{S}^{n+1}_{a(b)} \rangle$ (plaquette spins of two neighbouring plaquettes) versus J_p/J_d are shown in figure 8 and the spin correlations for large separations, namely $\langle \boldsymbol{S}^n_{a(b)} \cdot \boldsymbol{S}^{n+3}_\beta \rangle$ (dimer spin–plaquette spin), $\langle \boldsymbol{S}^n_{a(b)} \cdot \boldsymbol{S}^{n+3}_{a(b)} \rangle$ (plaquette spin–plaquette spin) and $\langle \boldsymbol{S}^n_\alpha \cdot \boldsymbol{S}^{n+3}_\beta \rangle$ (dimer spin–dimer spin) are given in figure 9.

In the dimer limit ($J_p \ll J_d$) the dimer and plaquette spins are decoupled; that is, $\langle \boldsymbol{S}^n_{\alpha(\beta)} \cdot \boldsymbol{S}^m_{a(b)} \rangle = 0$. Otherwise, the NN dimer correlation $\langle \boldsymbol{S}^n_\alpha \cdot \boldsymbol{S}^n_\beta \rangle$ takes its extreme value $-3/4$, while for spins belonging to different dimers, $\langle \boldsymbol{S}^n_{\alpha(\beta)} \cdot \boldsymbol{S}^m_{\alpha(\beta)} \rangle$ ($n \neq m$) goes

to zero, too. However, though the dimer and plaquette spins and the non-neighbouring dimer spins are not correlated, there is a well-pronounced correlation between more distant plaquette spins with several dimer spins in between. This is a typical quantum effect; a classical spin chain with NN exchange would be split into separate pieces at the point where the NN correlations are zero. The correlation between spins of different plaquettes is described by the effective Haldane chain (15); the numerical results indicate that this effective Hamiltonian describes the chain well until $J_p/J_d \sim 0.1$–0.15. For example for $J_p = 0.1J_d$ the plaquette–plaquette correlation $\langle \boldsymbol{S}^n_{a(b)} \cdot \boldsymbol{S}^m_{a(b)} \rangle$ differs from the corresponding Haldane correlation $\frac{1}{4}\langle \boldsymbol{S}_n \cdot \boldsymbol{S}_m \rangle$ (indicated by crosses in figure 7) by less than 3%.

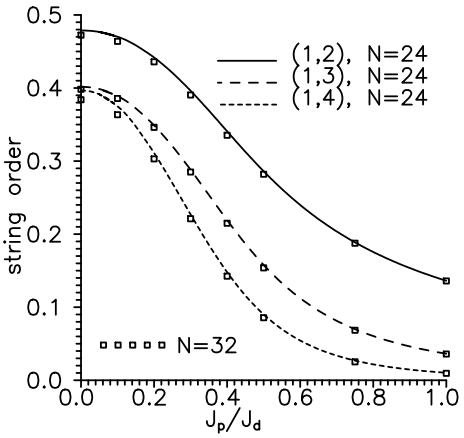

Figure 10. The string order $\mathcal{O}^z_\pi(n, m)$ (see equation (21)) for $(n, m) = (1, 2), (1, 3), (1, 4)$ versus J_p/J_d for the unfrustrated chains H_{p-d} of length $N = 24$ and $N = 32$.

In the plaquette limit ($J_p \gg J_d$) the ground state becomes a simple product state of the lowest four-spin plaquette states. Hence, for $J_p \to \infty$ we have $\langle \boldsymbol{S}^n_\alpha \cdot \boldsymbol{S}^m_\beta \rangle \to 0$, $\langle \boldsymbol{S}^n_{a(b)} \cdot \boldsymbol{S}^l_{a(b)} \rangle \to 0$ ($n \neq l$) and $\langle \boldsymbol{S}^n_\beta \cdot \boldsymbol{S}^n_{a(b)} \rangle \to -0.5$. For $J_p = J_d$ the pair correlation is already dropping down very rapidly (cf. figure 7) and, besides the correlation along the J_p-bond, $\langle \boldsymbol{S}^n_\beta \cdot \boldsymbol{S}^n_{a(b)} \rangle$, only extremely short-ranged correlations are present.

There is a comparably small region around $J_p/J_d \sim 0.3$–0.4 where we have a balance between J_p and J_d and all correlations are well pronounced. Since we have a gap for all $J_p > 0$ we argue that all correlations show exponential decay but with different correlation lengths ξ_{dd} for the dimer–dimer correlations, ξ_{dp} for the dimer–plaquette correlations and ξ_{pp} for the plaquette–plaquette correlations. The results obtained suggest that ξ_{pp} is quite large for $J_p/J_d \ll 1$ ($\xi_{pp} = \xi_{\text{Haldane}} \approx 6.03$ [18, 19, 21] for $J_p/J_d \to 0$). With increasing J_p there is a continuous decrease of ξ_{pp} up to $\xi_{pp} \to 0$ for $J_p \to \infty$. Otherwise, ξ_{dd} and ξ_{pd} are extremely small for $J_p/J_d \ll 1$ and $J_p/J_d \gg 1$ but show a maximum for $J_p/J_d \sim 0.35$ (ξ_{dd}) and $J_p/J_d \sim 0.3$ (ξ_{pd}) .

Finally we discuss the string order parameter describing possible hidden order in spin-1 chains [18–20]. This order parameter is defined as

$$\mathcal{O}^z_\pi(i, j) = \left\langle S^z_i \left(\exp \sum_{k=i+1}^{j} \mathrm{i}\pi S^z_k \right) S^z_j \right\rangle$$

where the S^z_i are spin-1 objects. For the Haldane spin-1 chain we have

$$\mathcal{O}^z_\pi = \lim_{|i-j|\to\infty} \mathcal{O}^z_\pi(i, j) = 0.374\,325\,096$$

and the value $\mathcal{O}_\pi^z(1,4)$ for the third neighbour is already close to $\mathcal{O}_\pi^z$ [18]. For the dimer plaquette chain considered we write

$$\mathcal{O}_\pi^z(n,m) = \left\langle S_{ab}^{n,z}\left(\exp\sum_{k=n+1}^{m} \mathrm{i}\pi S_{ab}^{k,z}\right)S_{ab}^{m,z}\right\rangle \tag{21}$$

with $S_{ab}^{m,z}$ defined in (3). The results are shown in figure 10. In agreement with pair correlation we observe a Haldane-like behaviour until $J_p/J_d \sim 0.1$–0.15 which is followed by a region $0.15J_d \lesssim J_p \lesssim 0.6J_d$ in which a crossover from the Haldane behaviour to the product state with vanishing pair correlations and vanishing string order takes place.

4. Conclusions

We have calculated the ground-state properties and low-lying excitations for an $S = 1/2$ chain with alternating dimers and plaquettes (see equations (1) and (2) and figure 1). This model is in some sense the 1D counterpart of the 1/5-depleted square-lattice Heisenberg model for CaV_4O_9.

While the classical ground state of the unfrustrated model H_{p-d} is the Néel state, there is a quantum competition between local singlet formation on the dimers and on plaquettes for $S = 1/2$. Beside giving exact-diagonalization and perturbation theory results, we have made several general and rigorous statements.

The main results can be summarized as follows. The ground-state properties and a class of excitations of H_{p-d} can be mapped onto a mixed spin-1/2–spin-1 chain with two dimer $S = 1/2$ spins and one effective $S = 1$ plaquette spin in the unit cell. In the limit of small plaquette bonds $J_p \ll J_d$, the ground-state correlations of the effective $S = 1$ plaquette spins can be described by a Haldane chain. On increasing the ratio J_p/J_d, a crossover takes place from the effective Haldane chain to a ground state described by a product of plaquette singlet states. The pair correlations are characterized by three different correlation lengths for dimer–dimer, dimer–plaquette and plaquette–plaquette correlations. In the limit in which $J_p \ll J_d$, the correlations between plaquette and dimer spins as well as between non-neighbouring dimer spins vanish, but surprisingly the correlations between plaquette spins are well pronounced. (Note that this is a purely quantum effect and has no classical analogue.) In the opposite limit, $J_p \gg J_d$, all of the correlation lengths are extremely short ranged.

Though the dimer–plaquette chain H_{p-d} is an $S = 1/2$ model, the first triplet excitation is separated by a gap for all parameter values except $J_p = 0$. This is consistent with the observation that the gapless ground state of the Bethe chain is quite unstable against the addition of relevant operators to create a gap in the excitation spectrum (see for instance the $S = 1/2$ chain with alternating NN bonds [38]).

Frustration can be introduced in the model in a simple way by adding an antiferromagnetic interaction of strength J_f between the top and the bottom spin of a plaquette (see (2) and figure 1). In the frustrated model we find a first-order quantum phase transition at a finite critical frustration J_f^c between the ground-state phase described above and a completely dimerized phase, which is similar to a recently described first-order transition in antiferromagnetic $S = 1/2$ coupled chains [29, 23]. Close to the transition the first excitation above the ground state is not a triplet but a singlet, which is a signature of strong frustration [37]. The model considered is one example showing rigorous validity of the Marshall–Peierls sign rule in a frustrated antiferromagnet.

As mentioned in section 2, we will briefly point out some important differences between the dimer–plaquette chain discussed in this paper and the spin-1/2 diamond chain considered

in [22, 23]. In the limit of small frustration the diamond chain corresponds to a quantum ferrimagnet. The ground state of this ferrimagnet has macroscopic total spin $S = N/6$, is long-range ordered and the spectrum is gapless [26–28]. On the other hand, the dimer–plaquette chain has a singlet ground state without long-range order and has a gap for all parameter values considered here. However, the common property of the two models consists in the product singlet state for large frustration.

Finally we mention that a straightforward extension of the model is obtained by adding further plaquette spins $\boldsymbol{S}_c^n$, $\boldsymbol{S}_d^n$, ... The ground-state properties of this extended model could be mapped onto a corresponding mixed spin-1/2–spin-$p/2$ chain (p is the number of spins in a plaquette n) with two dimer $S = 1/2$ spins and one effective $S = p/2$ plaquette spin in the unit cell.

Acknowledgments

This work was supported by the DFG (Ri 615/1-2) and the Bulgarian Science Foundation, Grant F412/94. The authors are indebted to U Schollwöck for fruitful discussions and to P Tomczak for reading the manuscript.

References

[1] Figuereido F, Karlhede A, Kivelson S, Sondhi S, Rocek M and Rokhsar D S 1990 *Phys. Rev.* B **41** 4619
Richter J 1993 *Phys. Rev.* B **47** 5794
Oitmaa J and Zheng Weihong 1996 *Phys. Rev.* B **54** 3022
[2] Taniguchi S, Nishikawa T, Yasui Y, Kobayashi Y, Sato M, Nishioka T, Kontani M and Sano K 1995 *J. Phys. Soc. Japan* **64** 2758
[3] Ohama T, Yasuoka H, Isobe M and Ueda Y 1997 *J. Phys. Soc. Japan* **66** 23
[4] Katoh N and Imada M 1995 *J. Phys. Soc. Japan* **64** 4105
[5] Ivanov N B, Krüger S E and Richter J 1996 *Phys. Rev.* B **53** 2633
[6] Albrecht M and Mila F 1996 *Phys. Rev.* B **53** R2945
[7] Troyer M, Kontani H and Ueda K 1996 *Phys. Rev. Lett.* **76** 3822
[8] Meshkov S V and Förster D 1996 *J. Phys.: Condens. Matter* **8** 7917
[9] Richter J and Ivanov N B 1996 *Proc. LT21 (Prague, 1996); Czech. J. Phys.* **46** 1919
[10] Ivanov N B and Richter J 1997 *Phys. Lett.* **232A** 308
[11] Bouloux J-C and Galy J 1973 *Acta Crystallogr.* B **20** 1335
[12] Starykh O A, Zhitomirsky M E, Khomski D I, Singh R R P and Ueda K 1996 *Phys. Rev. Lett.* **77** 2558
[13] Ueda K, Kontani H, Sigrist M and Lee P A 1996 *Phys. Rev. Lett.* **76** 1932
[14] Gelfand M P, Zheng Weihong, Singh R R P, Oitmaa J and Hamer C J 1996 *Phys. Rev. Lett.* **77** 2794
[15] White S R 1996 *Phys. Rev. Lett.* **77** 3633
[16] Sachdev S and Read N 1996 *Phys. Rev. Lett.* **77** 4801
[17] Bose I and Gosh A 1997 *Phys. Rev.* B **56** 3149
[18] White S R and Huse D A 1993 *Phys. Rev.* B **48** 3844
[19] Golinelli O, Jolicœur Th and Lacaze R 1994 *Phys. Rev.* B **50** 3037
[20] Mikeska H-J 1995 *Chaos, Solitons, Fractals* **5** 2585
[21] Kolezhuk A, Roth R and Schollwöck U 1997 *Phys. Rev.* B **55** 8928
[22] Takano K, Kubo K and Sakamoto H 1996 *J. Phys.: Condens. Matter* **8** 6405
[23] Niggemann H, Uimin G and Zittartz J 1997 *J. Phys.: Condens. Matter* **9** 9031
[24] Lieb E H and Mattis D C 1962 *J. Math. Phys.* **3** 749
[25] Klein D J 1982 *J. Chem. Phys.* **77** 3098
[26] Brehmer S, Mikeska H-J and Yamamoto S 1997 *J. Phys.: Condens. Matter* **9** 3921
[27] Pati S K, Ramasesha S and Sen D 1997 *J. Phys.: Condens. Matter* **9** 8707
[28] Ivanov N B 1997 *Preprint* cond-mat 9712014
[29] Xiang Y 1995 *Phys. Rev.* B **52** 12 485
[30] Valenti R, Stolze J and Hirschfeld P J 1991 *Phys. Rev.* B **43** 13 743
[31] Marshall W 1955 *Proc. R. Soc.* A **232** 48

[32] Kitatani H 1992 *Computational Approaches in Condensed-Matter Physics* ed S Miyashita, M Imada and H Takayama (Berlin: Springer) p 181
[33] Retzlaff K, Richter J and Ivanov N B 1993 *Z. Phys.* B **93** 21
[34] Richter J, Ivanov N B and Retzlaff K 1994 *Europhys. Lett.* **25** 545
[35] Zeng C and Parkinson J B 1995 *Phys. Rev.* B **51** 11 609
Bursill R, Gehring G A, Farnell D J J, Parkinson J B, Xiang T and Zeng C 1995 *J. Phys.: Condens. Matter* **7** 8605
[36] Voigt A, Richter J and Ivanov N B 1998 *Physica* A **245** 269
[37] Bernu B, Lecheminant P, Lhuillier C and Pierre L 1993 *Phys. Scr.* **49** 192
Bernu B, Lecheminant P, Lhuillier C, Pierre L, Sindzingre P, Waldtmann C and Everts H-U 1997 *Phys. Rev.* B **56** 2521
Lecheminant P, Bernu B, Lhuillier C, Pierre L and Sindzingre P 1997 *Preprint* cond-mat 9706167
[38] Gross M C and Fisher D S 1979 *Phys. Rev.* B **19** 402
Affleck I, Gepner D, Schulz H-J and Ziman T 1989 *J. Phys. A: Math. Gen.* **22** 511